

## Expression, Mutagenesis, and Characterization of Recombinant Low-Potential Cytochrome $c_{550}$ of Photosystem II<sup>†</sup>

Heather Andrews,<sup>‡</sup> Zhaoliang Li,<sup>‡</sup> Adriana Altuve-Blanco,<sup>§</sup> Mario Rivera,<sup>§</sup> and Robert L. Burnap<sup>\*‡</sup>

Department of Microbiology and Molecular Genetics, Oklahoma State University, Stillwater, Oklahoma 74078, and  
Department of Chemistry, University of Kansas, Lawrence, Kansas 66045

Received January 9, 2005; Revised Manuscript Received February 21, 2005

**ABSTRACT:** Cytochrome  $c_{550}$  of the photosystem II complex of cyanobacteria is an unusual member of the large protein family of monoheme  $c$ -type cytochromes. Despite the fact that it shares considerable amino acid sequence similarity and has a protein fold similar to the other members of the family, Cyt. $c_{550}$  has a midpoint potential ( $E_{m7} = -250$  mV) that is much lower than the positive midpoint potentials characteristic ( $E_{m7} = 100$ – $300$  mV) of this cytochrome family. An *E. coli* heterologous expression system involving secretion of the recombinant protein from *Synechocystis* PCC6803 to the periplasm was utilized to allow production of wild-type and mutant forms of the cytochrome. For most of the variants studied, the yield of protein was significantly enhanced by growth at 28 °C and inclusion of sucrose and betaine, in addition to isopropyl- $\beta$ -D-thiogalactoside (IPTG), to the growth medium of the *E. coli* expression host. Analysis of the protein products revealed that the wild-type protein maintained the redox and visible spectroscopic characteristics of the authentic protein. Mutations in the residues engaging in hydrogen bond interactions with the heme propionate (Asn49) and the axial 6th ligand His92 (Pro93) resulted in small (12–20 mV), but reproducible, upshifts in midpoint redox potential. Substitution of the axial ligand His92 with Met produced no discernible changes in the optical spectrum relative to the wild-type despite the fact that in this mutant, unlike the others studied here, the thioether linkage either was not formed or was highly labile as evidenced by loss of the heme during SDS–PAGE. On the other hand, the midpoint potential of the C550–H92M mutant was upshifted by approximately 70 mV. This value is significantly less of a perturbation than that observed in a similar mutant that is natively expressed in *Thermosynechococcus* but appears to have an intact thioether linkage between the heme and the polypeptide moiety.

Cytochromes are a diverse class of redox active molecules that function in a variety of electron transport processes ranging from aerobic respiratory chains to photosynthesis and reductive inorganic nutrient assimilation (1). The range of midpoint redox potentials (MP)<sup>1</sup> found in  $c$ -type cytochromes extends from  $-400$  to  $+400$  mV and, usually, can be functionally correlated with their respective roles in the various metabolic processes that they participate in. This large range in specific MP highlights the role of the protein in modulating the redox potential of the heme group (1). The polypeptide moieties of  $c$ -type cytochromes generally contain the consensus heme binding sequence, C-X-X-C-H, where the thiols of the cysteine (C) residues form covalent thioether linkages to the vinyl groups of the heme, the

imidazole nitrogen of the histidine (H) provides the fifth axial ligand to the heme iron, and X represents any residue. Only a few deviations from this consensus sequence have been found among the  $c$ -type cytochromes (2). Several subclasses of  $c$ -type cytochromes can be defined, depending on the nature of the sixth axial ligand residue of the heme iron atom. Typically, either a nitrogen atom of a histidine residue or a sulfur atom of a methionine residue fills the sixth ligand position of the heme iron atom. The differences in the electron donor–acceptor power (i.e., the electronegativity) between the ligands in the axial positions will influence the redox potential (1).

An interesting “natural experiment” on the role of the protein moiety on the redox characteristics of coordinated heme presents itself as the paralogous low-potential and high-potential  $c$ -type cytochromes in cyanobacteria. Redox characterization of these cytochromes shows that Cyt. $c_{550}$  is extremely more negative with a MP of  $-260$  mV (3–6) compared to the positive Cyt. $c_6$  with a MP of  $+314$  mV (7). In a case study, the low-potential Cyt. $c_{550}$  ( $E_{m7} = -260$  mV) and high-potential Cyt. $c_6$  ( $E_{m7} = +314$  mV) of the cyanobacterium *Arthrospira maxima* show uncanny structural similarities despite the redox differences as revealed in a recent X-ray crystallographic study (8). Both are monoheme cytochromes, and while Cyt. $c_6$  is composed of 89 amino acid residues, Cyt. $c_{550}$  is larger with 130 amino acid residues.

<sup>†</sup> This work was funded by the National Science Foundation (MCB-01323556 to R.L.B.) and the National Institute of Health (GM50503 to M.R.).

\* Corresponding author. Phone: 405-744-7445. Fax: 405-744-6790. E-mail: burnap@biochem.okstate.edu.

<sup>‡</sup> Oklahoma State University.

<sup>§</sup> University of Kansas.

<sup>1</sup> Abbreviations: betaine, (carboxymethyl)trimethylammonium; Cyt. $c_{550}$ , cytochrome  $c_{550}$ , an extrinsic protein of photosystem II complex encoded by *psbV*; EDTA, (ethylenedinitrilo)tetraacetic acid; Hepes, 4-(2-Hydroxyethyl)-1-piperazineethanesulfonic acid; IPTG, isopropyl- $\beta$ -D-thiogalactoside; MP, midpoint redox potential; PSII, photosystem II; SDS–PAGE, sodium dodecyl sulfate polyacrylamide gel electrophoresis; TMBZ, 3,3',5,5'-tetramethylbenzidine, used for staining heme.

Table 1: Oligonucleotide Primers Used for the Mutagenesis of the *psbV* Gene Encoding Cyt.*c*<sub>550</sub> of *Synechocystis* sp. PCC6803

mutation	primer pairs (forward and reverse)	restriction enzyme
T48I	F-5'GCACCCAATGTCACCTGCAGGGTAAAACCAAAATTAATAATAACG R-3'CGTGGGTACAGTGGACGTCCTTTTGGTTTAAATTATTATTGC	<i>Pst</i> I
L91I	F-5'-CTATTCGAAATACATCCCAATATTCTAGACCCGACATCTAC R-3'-GATAAGCCTTTATGTAGGGTTATAAAGATCTGGGCTGTAGATG	<i>Xba</i> I
P93A	F-5'-GACTATTCGGAGCTCCATGCCAATATTTCC R-3'-CTGATAAGCCTCGAGGTACGGTTATAAAGG	<i>Sac</i> I
N49L	F-5'-CCAATGTCACCTGCAGGGTAAAACCAAAACTCTTAATAACGTTAG R-3'-GGTTACAGTGGACGTCCTTTTGGTTTGAATTATTGCAATC	<i>Pst</i> I
N49D	F-5'-CCAATGTCACCTGCAGGGTAAAACCAAAACTGATAATAACGTTAG R-3'-GGTTACAGTGGACGTCCTTTTGGTTTGAATTATTGCAATC	<i>Pst</i> I
H92M	F-5'-GACTATTCGGAGCTCATGGCCAATATTTCC R-3'-CTGATAAGCCTCGAGTACCGGTTATAAAGG	<i>Sac</i> I

Nevertheless, the extensive regions of sequence similarity, adjacency on the genome, and highly similar folds have led to the suggestion that Cyt.*c*<sub>550</sub> and Cyt.*c*<sub>6</sub> have descended from the same ancestral cytochrome but have since diverged to structures that provide for the nearly 575 mV difference in MPs. In addition to sharing sequence similarity, Cyt.*c*<sub>550</sub> also shares some structural similarity with Cyt.*c*<sub>6</sub>. Comparison of the two 3-D structures suggests that the difference in midpoint might be attributed to any or all of the following factors: solvent exposure of the heme, electrostatic environment of the heme propionates, and/or heme–iron ligation. A prominent difference between Cyt.*c*<sub>550</sub> and Cyt.*c*<sub>6</sub> is the nature of the axial sixth ligand, which is His92 in Cyt.*c*<sub>550</sub> and Met61 in Cyt.*c*<sub>6</sub>. Cytochromes with His–Met axial coordination have redox values ranging from +400 to 0 mV, while bishistidine coordinated cytochromes typically have potentials ranging from 0 to –400 mV (1, 9). However both cytochromes, *c*<sub>550</sub> and *c*<sub>6</sub>, do have the C–X–X–C–H (C = cysteine, H = histidine, X = any residue) heme consensus binding sequence. Both cytochromes also have the evolutionarily conserved proline residue at position 93, which in the case of Cyt.*c*<sub>550</sub> orients its carbonyl oxygen to form a hydrogen bond with the Nδ atom of the axial His92 heme ligand. In addition to having a different sixth axial ligand, Cyt.*c*<sub>550</sub> has an additional N-terminal 22 residues as compared to Cyt.*c*<sub>6</sub>. Also, there is an insert in the primary structure of Cyt.*c*<sub>550</sub> that is not found in Cyt.*c*<sub>6</sub> between residues 89 and 103. Despite its larger mass, Cyt.*c*<sub>550</sub> actually folds into a structure with larger solvent accessibility to the surface of the heme (9.7% exposure) compared to the Cyt.*c*<sub>6</sub> fold (6.6% exposure). The great solvent exposure may account, in part, for its lower redox potential (9, 10). Another unresolved question concerns the role of the thioether linkage found in *c*-type cytochromes (2). Biogenesis of the *c*-type cytochromes requires specialized enzymatic machinery to catalyze the formation of the thioether linkages (11). Presently, the biological function of the thioether linkage remains unresolved, although some evidence suggests that the role may be stabilization of structure rather than tuning of the redox potential.

From a functional perspective, the low-potential Cyt.*c*<sub>550</sub> remains a puzzle since this cytochrome is intimately associated with the photosynthetic H<sub>2</sub>O oxidation complex, which operates at extremely oxidizing potentials. Extensive research has established that it does not participate in the main photosynthetic reactions despite its close proximity to the major cofactors in this process, and thus, a function other than a structural component of the H<sub>2</sub>O oxidation complex

remains to be established. In the present study we describe a heterologous expression system for Cyt.*c*<sub>550</sub> and present the characterization of several Cyt.*c*<sub>550</sub> mutants aimed at understanding the factors controlling the redox potential of the heme of Cyt.*c*<sub>550</sub> of the cyanobacterium *Synechocystis* sp. PCC6803 (hereafter, *Synechocystis*).

## MATERIALS AND METHODS

**Construction of a Heterologous Cyt.*c*<sub>550</sub> Expression System.** The coding sequence of mature Cyt.*c*<sub>550</sub> from *Synechocystis* sp. PCC6803 was amplified by PCR using *Pfu*Turbo polymerase (Stratagene, La Jolla, CA). The forward primer 5' GCT CCC ATG GTG GAG TTA ACC GAA AGC 3' which introduced a *Nco*I site (in bold) and the reverse primer 5' GCG CGG ATC CCT AGA AGT AGA TGG TGC C 3' which introduced a *Bam*HI site (in bold) were used to amplify the encoding sequence of mature Cyt.*c*<sub>550</sub>. The PCR product was inserted into the *Nco*I and *Bam*HI sites of the pET-22b (+) vector (Novagen, Madison, WI) to create expression plasmid pET22bC550 (pETC550). A similar strategy was used to generate plasmids having either an amino- or carboxy-terminal hexahistidine (H6) affinity tag. The resultant plasmids were used to transform the *E. coli* expression strain, BL-21(DE3) that also contained plasmid pEC86 (12) (a kind gift from Prof. Linda Thony-Myer, Swiss Federal Institute of Technology, Zurich), which facilitates the maturation process involving attachment of the heme to the apoprotein.

**Site-Directed Mutagenesis.** Specific amino acid substitutions were introduced into the *psbV* coding sequence using the Stratagene QuikChange (La Jolla, CA) protocol. Mutagenic primer pairs were designed according to the manufacturer's recommendations such that each primer was between 30 and 45 bases in length with a GC content of at least 40% (Table 1). Each primer contained at least 10–15 bases of correct sequence on both sides of the engineered mutation and terminated in one or more G or C bases. A silent mutation was also introduced into each of the primers to add an additional restriction enzyme cut site for verification of the mutation after transformation. The DNA oligonucleotide primers were synthesized in approximately 100 nmole batches obtained from Integrated DNA Technologies, Inc. (Coralville, Iowa). Each primer was 5'-phosphorylated and was purified by the manufacturer by polyacrylamide gel electrophoresis (PAGE).

**The Overexpression of pETC550 in BL-21(DE3) *E. coli* with pEC86.** Starter cultures were grown overnight with

shaking at 250 rpm at 28 °C in Terrific Broth (TB) (13) containing chloramphenicol (30  $\mu\text{g/mL}$ ) and ampicillin (100  $\mu\text{g/mL}$ ) and were then used to inoculate 1 L (5 mL starter culture) of the same medium supplemented with 300 mM sucrose and 2.5 mM betaine in 4 L Erlenmeyer flasks. The cultures were grown with shaking (250 rpm) at 28 °C until reaching an  $\text{OD}_{600} = 0.8\text{--}1.0$  upon which 0.5 mM IPTG was added to induce expression of cytochrome. The induction was allowed to proceed in the shaker for approximately 4 h. Cell cultures were placed at 4 °C overnight for preparation of the periplasmic fraction the following day.

**Purification of Cyt.*c*<sub>550</sub>.** Recombinant Cyt.*c*<sub>550</sub> was recovered in host cell periplasmic fraction as prepared according to ref 14. Further purification of the cytochrome was achieved using the chromatographic procedures described by Ho et al. (15) with modifications. The periplasmic fraction was applied to a DEAE cellulose column (2.6 cm  $\times$  20 cm), and Cyt.*c*<sub>550</sub> was eluted with a 0–500 mM NaCl gradient. Fractions containing Cyt.*c*<sub>550</sub> were pooled and concentrated to about 15 mL by ultrafiltration (Amicon model 8200 with YM10 membrane) and then were loaded onto a DEAE Sephacel column (1.6 cm  $\times$  20 cm) by 10-fold dilution; Cyt.*c*<sub>550</sub> was eluted with a 150–500 mM NaCl gradient, and fractions containing Cyt.*c*<sub>550</sub> were pooled and concentrated to 3 mL by ultrafiltration. Finally, Cyt.*c*<sub>550</sub> was applied to a Sephadex G-75 column (1.6 cm  $\times$  40 cm) and eluted by 50 mM Tris-HCl, pH 8.0. Cyt.*c*<sub>550</sub> fractions were pooled and concentrated by ultrafiltration and dialyzed against 50 mM MES/NaOH (pH 6.5). His-tagged Cyt.*c*<sub>550</sub> was purified by Ni-NTA Superflow affinity chromatography (Qiagen). The periplasmic fraction from 4 L of culture was mixed with 10 mL preequilibrated Ni-NTA Superflow and incubated on ice for 1 h with gentle shaking occasionally, then the resin was packed into a column. The column was washed with 6 vol of washing buffer A (50 mM Tris-HCl, pH 8.0, 300 mM NaCl, and 10 mM imidazole). His-tagged Cyt.*c*<sub>550</sub> was eluted with 6 vol of elute buffer (50 mM Tris-HCl, pH 8.0, 300 mM NaCl, and 250 mM imidazole). Finally, the His-tagged Cyt.*c*<sub>550</sub> was concentrated by ultrafiltration (Amicon model 8200 with YM10 membrane) and dialyzed against 50 mM MES/NaOH (pH 6.5), then stored at –80 °C until further use.

**Analytic Methods.** The spectra of Cyt.*c*<sub>550</sub> were obtained using UV–VIS Scanning Spectrophotometer (Shimadzu), and quantitation of cytochrome was calculated using an extinction coefficient of  $25 \times 10^3 \text{ M}^{-1} \text{ cm}^{-1}$  at 549 nm with an excess of reductant (dithionite) according to Navarro et al. (6). Denaturing sodium dodecyl sulfate polyacrylamide electrophoresis (SDS–PAGE) was conducted using the Laemmli system supplemented with 6 M urea. Staining for heme was conducted by preparing 20 mL of 3',3',5',5'-tetramethylbenzidine (TMBZ) gel soak solution made by dissolving 26 mg of TMBZ in 0.5 mL of DMSO. Then, 4.0 mL of 95% ethanol and 100% glacial acetic acid and 5.5 mL of water were added to the TMBZ/DMSO soak solution. The SDS–PAGE gel was then soaked in the TMBZ solution for 1 h at room temperature with gentle agitation. The staining reaction was then initiated by adding  $\text{H}_2\text{O}_2$  to 1% v/v. The reaction was then monitored for the visible blue bands. Once the blue bands were detected, the SDS–PAGE could be viewed for the respective single band representing each purified cytochrome.

**Redox Titrations.** Redox titrations for Cyt.*c*<sub>550</sub> were conducted using a custom-made cell with a quartz cuvette (1.0 cm path-length) that contained a platinum foil working electrode, a Ag/AgCl reference electrode, and a magnetic stirrer modeled after the apparatus published by Stankovich (16). The cell was fused to a custom-made set of gas ports through a gradient coupling. A Rotaflo stopcock attached to a Schlenk line served as an inlet for argon to keep the inside of the cell oxygen free. The small port in the front of the cell allowed addition of mediators and protein and was filled with a rubber septum prior to the onset of the titrations. All redox values are expressed relative to a normal hydrogen electrode. Redox mediators were each added at 20  $\mu\text{M}$ : 1,2-naphthoquinone,  $E_{\text{m}7} = 157 \text{ mV}$ ; tolulene blue,  $E_{\text{m}7} = 115 \text{ mV}$ ; duroquinone,  $E_{\text{m}} = -5 \text{ mV}$ ; pentaaminechlororuthenium(III) dichloride,  $E_{\text{m}} = -40 \text{ mV}$ ; 2,5-dihydroxy-*p*-benzoquinone,  $E_{\text{m}7} = -60 \text{ mV}$ ; 2-hydroxy-1,4-naphthoquinone,  $E_{\text{m}7} = -130 \text{ mV}$ ; anthraquinone-2,6-disulfonic acid,  $E_{\text{m}7} = -180 \text{ mV}$ ; anthraquinone-2-sulfonic acid,  $E_{\text{m}7} = -250 \text{ mV}$ ; methyl viologen,  $E_{\text{m}7} = -440 \text{ mV}$ ; lumiflavine,  $E_{\text{m}7} = -510 \text{ mV}$  in a buffer consisting of 200 mM sodium phosphate buffer volumetrically adjusted with mono- and dibasic salts to pH 7.0. This solution was bubbled with argon for 45 min, and then 10  $\mu\text{M}$  of protein was added to the cell with a Hamilton gastight syringe and the cell was sealed with a septum. After the cell was pumped and purged with argon 3–4 times to remove dissolved oxygen, the titrations were carried out by adding the appropriate amount of a 1 mM solution of sodium dithionite by syringe, while simultaneously monitoring the UV–VIS spectrum of the protein using a diode array spectrophotometer (Ocean Optics) and following shifts at 550 nm and taking the corresponding potentials with the voltmeter. Absence of hysteresis was confirmed by reoxidation of reduced samples using potassium ferricyanide.

## RESULTS

**Binary Expression System for *Synechocystis* sp. PCC6803 Cytochrome *c*<sub>550</sub>.** To facilitate the preparation of recombinant Cyt.*c*<sub>550</sub>, a strain of *E. coli* was constructed that contains two distinct plasmids. The first plasmid, pETC550, allows heterologous expression in *E. coli* under the control of a T7 promoter with the *pelB* signal sequence directing the protein to the periplasmic space with its concomitant proteolytic removal by the signal peptidase. The second plasmid of the binary system, pEC86, contains genes involved in biogenesis of *c*-type cytochromes (12). The best yields for the recombinant cytochromes were obtained using a buffered rich medium, Terrific Broth (TB) supplemented with sucrose and betaine (17, 18) with growth at 28 °C. These conditions gave yields in the range of 2.6–4.0 mg/L of crude protein and 1.7–3.3 mg/L of purified protein. All forms of the recombinant cytochromes exhibited higher yields with sucrose and betaine, although the effect was most dramatic for C550–H92M. When the growth medium was supplemented with 2.5 mM betaine and 300 mM sucrose and cultures were induced with 0.5 mM IPTG at 28 °C, we saw a 4-fold increase in the expression of C550–H92M as compared to the control under the same conditions, but without betaine or sucrose (data not shown). The improvements in yield were additive but with sucrose having the greatest effect. The recombinant proteins were isolated from *E. coli* host cells



Table 2: Summary of the Physiochemical Properties of Recombinant Cyt.*c*<sub>550</sub> and Its Mutants

cytochrome	average midpoint potential <sup>a</sup>	potential difference from wild-type	absorption maximum, $\gamma$ <sup>b</sup>	absorption maximum, $\beta$ <sup>c</sup>	absorption maximum, $\alpha$ <sup>d</sup>
C550 wild-type	-254 ± 2	0	417.6 (406.6)	522.5	550.6
C550-NtermH6	-243 ± 3	11	417.6 (406.6)	522.5	550.6
C550-CtermH6	-248 ± 5	6	417.6 (406.6)	522.5	550.6
C550-T48I	-253 ± 1	1	417.6 (406.6)	522.5	550.6
C550-N49D	-242 ± 6	12	417.6 (406.6)	522.5	550.6
C550-N49L	-235 ± 1	18	417.6 (406.6)	522.5	550.6
C550-L91I	-251 ± 1	3	417.6 (406.6)	522.5	550.6
C550-H92M <sup>e</sup>	-185 ± 9	69	416.5 (408.5)	522.5 (529)	551.0
C550-P93A	-235 ± 5	19	417.6 (406.6)	522.5	550.6
<i>Thermosynechococcus</i> <sup>f</sup> C550 wild-type	-270	0	nd <sup>g</sup>	523.0	549.0
<i>Thermosynechococcus</i> <sup>f</sup> C550-H92M	-140	130	nd <sup>g</sup>	nd <sup>g</sup>	552.0
<i>Thermosynechococcus</i> <sup>f</sup> C550-H92C	-300	-30	nd <sup>g</sup>	nd <sup>g</sup>	552.0

<sup>a</sup> The average potential, standard deviation, and difference in redox potential from the wild-type redox potential. <sup>b</sup> The absorbance maxima in the Soret region observed for the reduced and oxidized (parentheses) cytochromes as described in Figure 2 and the Materials and Methods. <sup>c</sup> As *b*, but for  $\beta$  region. <sup>d</sup> As *b*, but for  $\alpha$  region. <sup>e</sup> Heme was not covalently linked in the recombinant protein (this work), but it is formed when the mutation is expressed in the native system (36). <sup>f</sup> Taken from the work of Roncel (5), Kirolovsky (20), and colleagues. <sup>g</sup> nd = not determined.

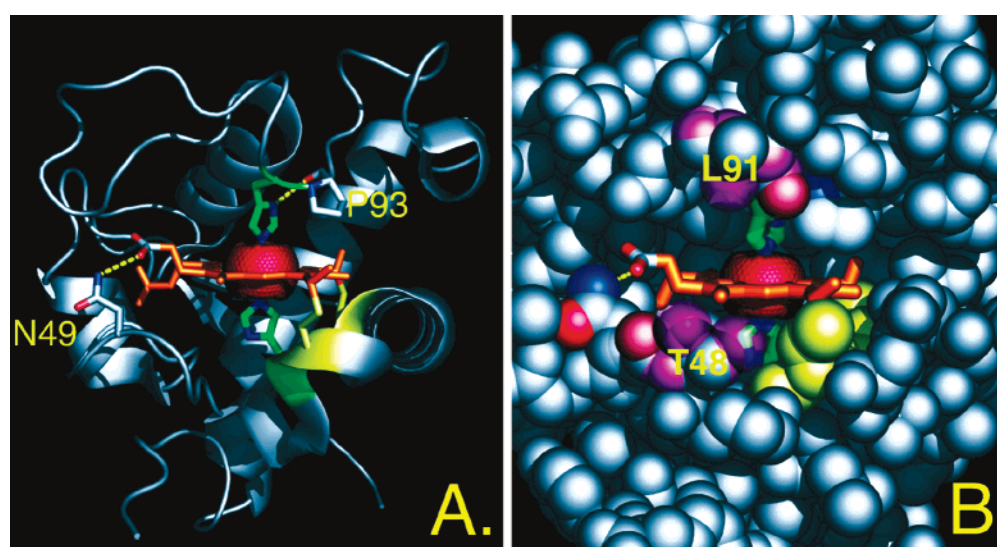


FIGURE 1: (A) *Synechocystis* sp. PCC6803 cytochrome *c*<sub>550</sub> axial coordination of the heme (orange), iron (red), and the polar contacts that have been mutated. Note the wild-type bishistidine (His41 and His92) axial ligation of the heme iron. The main chain carbonyl of Pro93 forms a hydrogen bond with the (imidazole) Nδ atom of His92 shown by the yellow dashed line. The hydrogen bond formed between Asn49's side chain amide to the heme propionate D oxygen atom is also indicated by yellow dashed line. The thioether covalent linkage between Cys37, Cys40 (yellow), and the heme porphyrin is not formed in the recombinant axial ligand mutant C550-H92M, but is formed when the mutation is expressed in the native system (36). (B) A space-filling representation depicting the exposed heme edge of the cytochrome viewed from the same perspective as in A. Leucine 91 (L91) and threonine 48 (T48) were separately targeted for mutagenesis with isoleucine substitutions to occlude access of solvent water. The modeled volumes of the substituting leucines are indicated with the semitransparent red spheres. Models were constructed using Insight II (Accelrys) and using the Discover module. Figures were rendered using PyMOL, DeLano Scientific, <http://www.pymol.org>.

by extraction of the periplasmic fraction and purification by a combination of ion exchange and gel permeation chromatography. Formation of a thioether covalent linkage occurs in all cases except the C550-H92M mutant as determined by TMBZ heme-staining of SDS-PAGE/6 M urea gels. Nickel-chelate affinity chromatography was used in the case of the His-tagged versions of the protein, C550-NtermH6 and C550-CtermH6.

**Site-Directed Mutagenesis.** The plasmid pETC550 allowed the efficient construction of oligonucleotide directed mutations using standard PCR-based procedures (see Materials and Methods) and posed no unusual complications. The following mutations were constructed: (1) The H-bond interaction between the heme D ring propionate oxygen and the side chain amide nitrogen of asparagine 49 was modified by substituting asparagine 49 with aspartate and leucine

producing C550-N49D and C550-N49L, respectively. (2) Reduction of the solvent exposure of the heme C and D ring at the open cleft of the heme binding site were attempted by substitutions of threonine 48 and leucine 91, each with isoleucine, to produce C550-T48I and C550-L91I, respectively. (3) The distal axial ligand, histidine 92, was substituted with methionine (C550-H92M), and the highly conserved proline 93, which engages in an H-bond via its carbonyl oxygen to the imidazole Nδ of histidine 92, was replaced with an alanine (C550-P93A) which is expected to distort that H-bond. Figure 1 illustrates several of the sites of amino acid substitution that were investigated.

**Visible Spectroscopy.** Figure 2 shows typical visible spectra of reduced and oxidized cytochrome for Cyt.*c*<sub>550</sub> and the Cyt.*c*<sub>550</sub> His92 ⇒ Met92 axial ligand mutant (C550-H92M). The Soret band of the reduced Cyt.*c*<sub>550</sub> has a peak

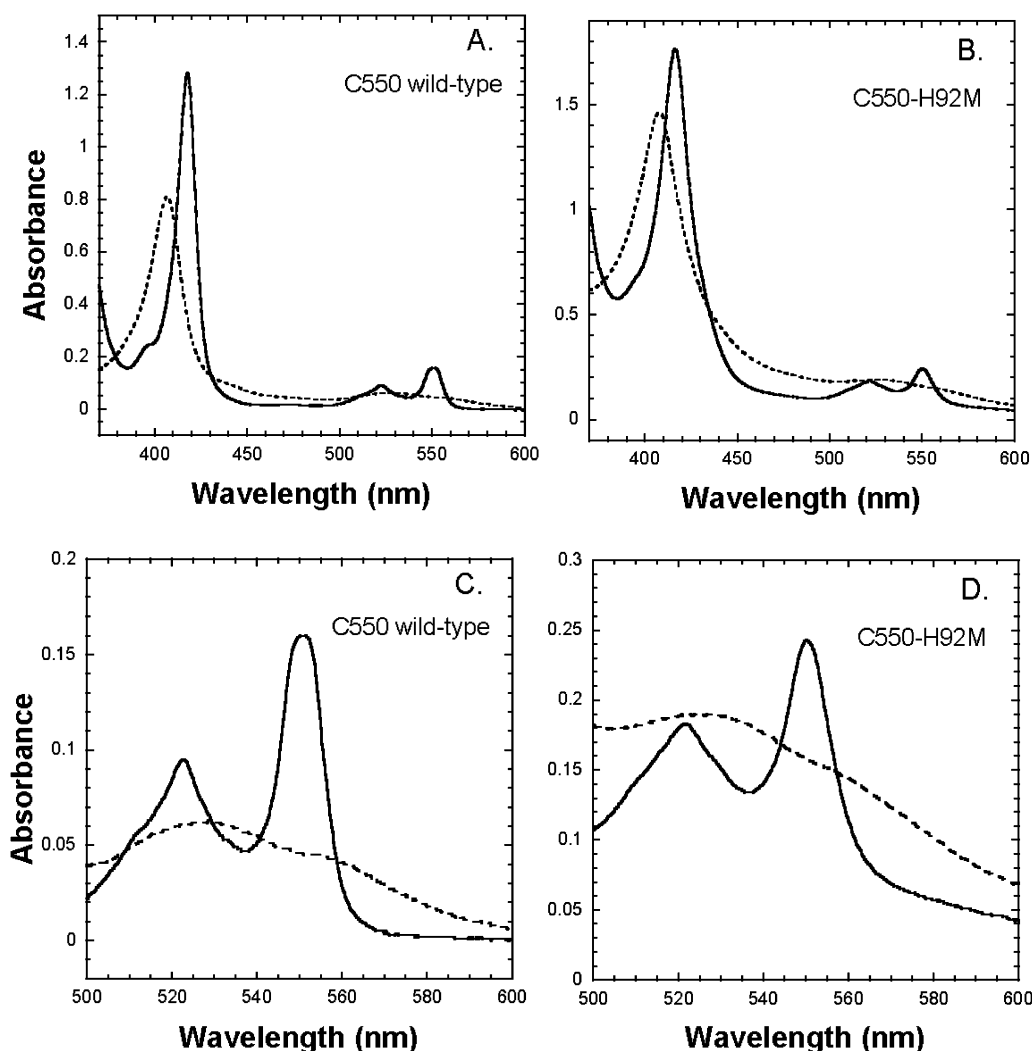


FIGURE 2: Visible spectra of reduced (solid lines) and oxidized (dashed lines) recombinant wild-type Cyt.*c*<sub>550</sub> (A and C, C550-wild-type,) and the Cyt.*c*<sub>550</sub> His92 → Met92 axial ligand mutant (B and D, C550–H92M) expressed in *E. coli*. (A and B) The  $\alpha$ ,  $\beta$ , and Soret bands (see Table 2 for wavelengths of the peak maxima). (C and D) The expanded region containing the  $\alpha$  and  $\beta$  peaks. Reduction of the cytochrome was obtained using sodium dithionite, whereas the fully oxidized cytochrome was observed under ambient solution conditions (spectra were essentially identical to those obtained by chemical oxidation with potassium ferricyanide (not shown)).

near 417 nm, an  $\alpha$ -band peak near 550 nm, and a  $\beta$ -band peak near 522 nm (Figure 1). These values closely agree with the values obtained for the authentic *Synechocystis* sp. PCC6803 Cyt.*c*<sub>550</sub> by Navarro et al. (6). The spectral characteristics of these and the other mutant cytochromes expressed in *E. coli* are summarized in Table 2. Apart from the small differences seen in the C550–H92M mutant, the spectra of the other mutant cytochromes were indistinguishable from the wild-type. Notably, the mutant does not exhibit a charge–transfer band in the 690–700 nm region (not shown) that is characteristic of *c*-type cytochromes His–Met axial ligation. However, this absence does not preclude ligation of the heme by the substituting methionine (19). As discussed below, the absence of a spectral shift in the C550–H92M mutant contrasts with results obtained for the corresponding His92 → Met92 mutant expressed in its native cyanobacterial genetic background (20).

**Cyt.*c*<sub>550</sub> Does Not Exhibit Reactivity with Small Ligands.** Since a possible *in vivo* function of Cyt.*c*<sub>550</sub> is to react with radical species generated during the course of the redox reactions of photosystem II, the ability of the heme to undergo ligand exchange was explored. To test if CO reacts

with Cyt.*c*<sub>550</sub>, the spectra of the reduced Cyt.*c*<sub>550</sub> were obtained under bubbling with CO. However, no difference was observed indicating that the ligands of the heme are stable and cannot be replaced by CO. Also, we investigated the effect of sodium cyanide on the spectra of the oxidized Cyt.*c*<sub>550</sub> in buffers set at different pHs (pH 3.5–8.5) to probe whether potential protonation of the His ligands could result in more facile ligand replacement, yet no differences were observed. Taken together, the results suggest that the ligation of the heme group is very stable and the cytochrome is unlikely to react with alternative ligands under physiological conditions.

**Redox Midpoint Potentials of the Wild-Type and Mutant Cyt.*c*<sub>550</sub>.** Characteristic sigmoidal titration plots were observed for recombinant wild-type *Synechocystis* sp. PCC6803 Cyt.*c*<sub>550</sub> and its mutant derivatives as shown in Figure 3 and summarized in Table 2. The average MP determined for the wild-type Cyt.*c*<sub>550</sub> was  $-254 \pm 2$  mV versus NHE, which is in agreement with previously published redox values for authentic Cyt.*c*<sub>550</sub> isolated from *Synechocystis* sp. PCC6803 (4, 6) and from *Thermosynechococcus elongatus* (5). Interestingly, the addition of the His6 affinity purification tag on

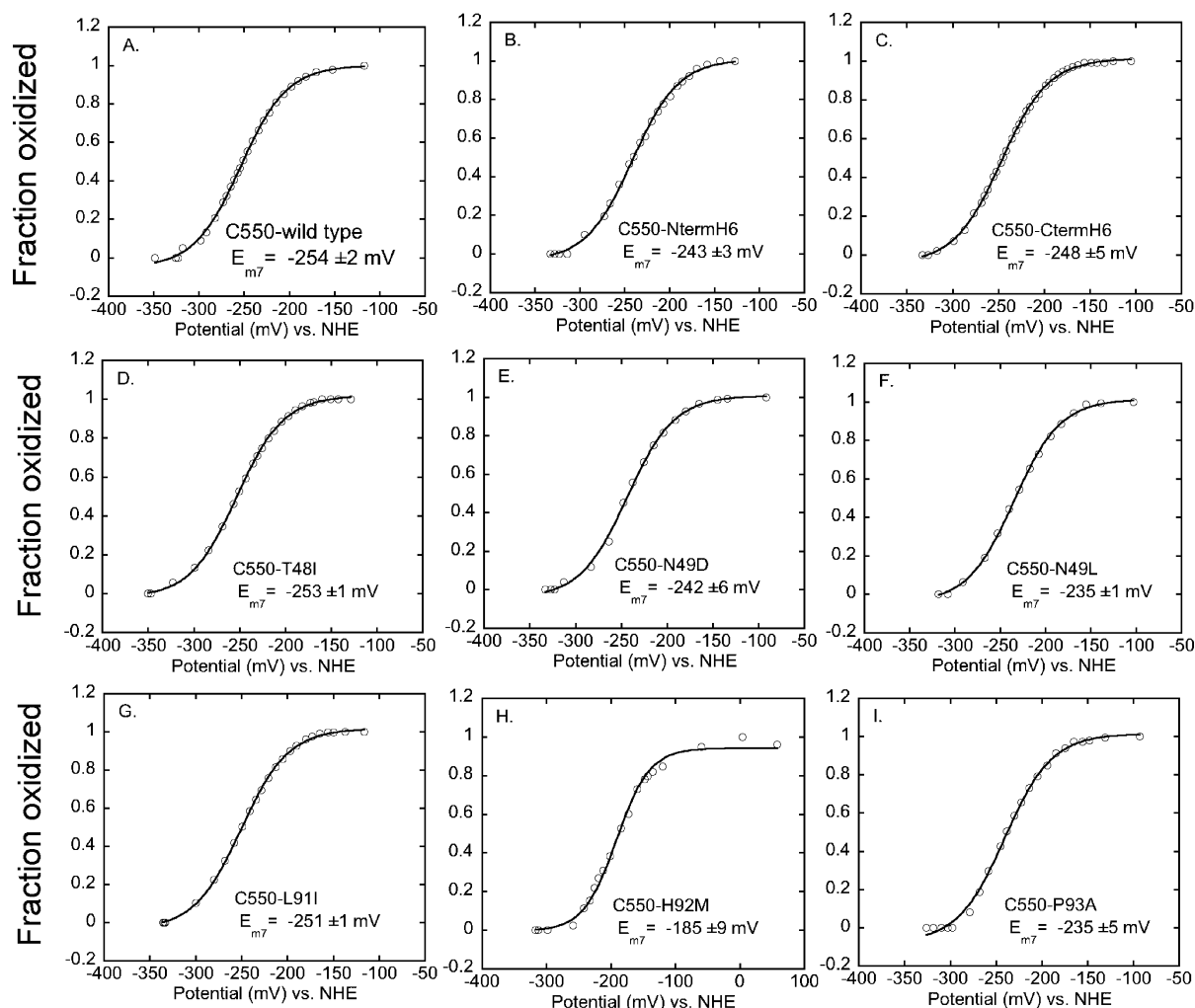


FIGURE 3: Reductive titrations of recombinant *Synechocystis* sp. PCC6803 wild-type Cyt.*c*<sub>550</sub> and its mutant derivatives. All titrations were carried out with  $\sim 10 \mu\text{M}$  protein in 200 mM sodium phosphate buffer, pH 7.0, at 24 °C. The titrations were monitored by following the intensity of the absorbance of the oxidized  $\alpha$ -band (550 nm) of the cytochrome and the equilibrium potential resulting from each addition of sodium dithionite in the presence of redox mediators (see Materials and Methods). The data were fit using the Nernst equation assuming one electron processes ( $n = 1$ ), based upon separate log transform plots of the data which produced best fits with a slope approaching 59 mV. The data and fits shown here are for a single representative titration of each cytochrome. There were at least three titrations performed per cytochrome, and the numerical values are the average and standard deviations for dataset of each cytochrome.

either the amino or the carboxy end of the otherwise wild-type cytochrome produced slight upshifts in redox potential.

The mutation producing the largest impact upon the MP was the substitution of the axial heme ligand His92 with the methionine (C550–H92M), which resulted in an approximately 70 mV upshift in potential to  $-185 \pm 9$  mV versus NHE. The C550–P93A mutation yielded a protein with a MP of  $-235 \pm 5$  mV versus NHE as shown in (Figure 3). This value was different from the wild-type Cyt.*c*<sub>550</sub> by 19 mV. Although proline 93 forms a hydrogen bond to the N $\delta$  atom of His92, upon the substitution of proline 93 for an alanine, the hydrogen bond may not be lost since it involves the peptide backbone carbonyl of the proline. Therefore the impact on MP is more likely due to changes in H-bonding orientation or length. The C550–N49L and C550–N49D mutants were produced to impact the H-bond between the amide nitrogen of the asparagine 49 with the propionate of the D ring of the heme moiety. The MPs of C550–N49L and C550–N49D were  $-235 \pm 1$  and  $-242 \pm 6$  mV, upshifts from the wild-type midpoint of 18 and 12 mV, respectively. Neither of the mutations designed to reduce the solvent exposure and polarity of the heme edge, C550–T48I

and C550–L91I, produced a large change in the MP relative to the wild-type. The C550–T48I and C550–L91I exhibited MPs of  $-253 \pm 1$  and  $-251 \pm 1$  mV versus NHE compared to the  $-254 \pm 2$  mV of the wild-type.

## DISCUSSION

Cyanobacterial Cyt.*c*<sub>550</sub> contains a monoheme with low-spin bishistidine coordination and possesses an unusually low midpoint redox potential (3–6, 20–22). Although other *c*-type cytochromes have even lower MPs, Cyt.*c*<sub>550</sub> has the lowest MP of any monoheme *c*-type cytochrome examined to date and thus is an excellent model for probing the structural factors modulating redox potential. Here we describe the development of a heterologous *E. coli* expression system for Cyt.*c*<sub>550</sub> and its utilization to address questions on the role of specific amino acids in producing the very low MPs observed for this unusual cytochrome.

**Expression of Recombinant Cyt.*c*<sub>550</sub>.** The basic strategy for the expression of *c*-type cytochromes using a binary expression system involving one plasmid encoding a periplasmically directed cytochrome apoprotein and a second



plasmid producing factors for the transport and attachment of the heme moiety was developed by Thony-Meyer (23, 24) and used for the production of another cyanobacterial cytochrome, cytochrome *m*, previously (14). The binary plasmid expression system allowed the production of low-potential Cyt.*c*<sub>550</sub> at levels comparable to that achieved previously by this type of system and by other expression systems (25), although lower than other strategies for the expression of *c*-type (26) and *b*-type (27) cytochromes. The recombinant wild-type Cyt.*c*<sub>550</sub> has physiochemical characteristics that are indistinguishable from the authentic native cytochrome purified from *Synechocystis* sp. PCC6803 extracts (6). Optical and redox properties of the C550-wild-type were virtually identical to the previously reported characteristics for the authentic cytochrome isolated from *Synechocystis* sp. PCC6803 (6) and, likewise, similar to other cyanobacterial Cyt.*c*<sub>550</sub> homologues including the extensively characterized versions from *Thermosynechococcus* (5). This indicates that the same protein fold and similar hydrogen bonding interactions are present in the *E. coli*-expressed protein, as are present in the native *Synechocystis* Cyt.*c*<sub>550</sub>. Furthermore, the formation of the thioether linkage occurred in all the cytochrome variants, except C550–H92M, as evidenced by SDS–PAGE of the protein.

**H-Bonding to Heme Propionate.** An important factor in controlling the MP of cytochromes is the state of the propionate carboxylate groups of the C and D rings of the heme. The redox potential of the heme is influenced by the degree of ionization, the H-bonding partners, the orientation of the carboxylate moiety, and the extent of solvation of the propionate (9, 28). The influence of negative charge on the ionized propionates in favoring the oxidation of the heme is demonstrated by elimination of the charge through substitution with the dimethyl ester form of the heme (29, 30). In cyanobacterial Cyt.*c*<sub>6</sub>, evolutionarily related to Cyt.*c*<sub>550</sub> (discussed in the introduction section), the propionate oxygen atoms are hydrogen-bonded to the positively charged Lys 29 and Lys 59 (8, 31). This positive charge may help to stabilize the electron gained by reduction of the heme and thus lead to the higher MP of Cyt.*c*<sub>6</sub> as compared to Cyt.*c*<sub>550</sub>. In Cyt.*c*<sub>550</sub>, the propionate of the C ring is buried within the heme-binding cleft where it interacts with a guanidino nitrogen of arginine 66 and engages in H-bonding a backbone carbonyl. The propionate of the D ring, on the other hand, protrudes from the cleft and, in the crystal structure, engages in H-bonding with the side chain amide of asparagine 49 (2.76 Å bond length), as well as with two water molecules. Substitution of this asparagine with aspartate (C550–N49D) and with leucine (C550–N49L) each produced upshifts of 12 and 18 mV, respectively (Table 2). A mutagenesis study of mitochondrial cytochrome *c* has shown that substitutions decreasing the electron-withdrawing character of a side chain in proximity to a propionate group decrease the MP of the heme (32). With this in mind, it may have been expected that the substitution of the H-bonding asparagine with a leucine in the C550–N49L mutant would decrease rather than increase the MP as observed. Likewise, substitution with the aspartic acid might be expected to decrease the potential by increasing the density of negative charge in that region. Neither of these situations seems to have occurred. On the other hand, it may be more likely that the H-bond between the asparagine and the propionate may orient the propionate

in a manner that increases the effect of the charge of the ionized propionate on the heme iron and this orienting effect is lost in both types of substitution.

**Solvent Access.** Solvent accessibility of the heme prosthetic group is known to play a role in modulating the redox potential of the heme. The loss of solvation energy by moving the heme out of the high dielectric of water into the relatively low dielectric of the protein environment destabilizes the oxidized state more than the reduced state making the midpoint more negative (9, 10, 33). Considerably higher redox potentials for Cyt.*c*<sub>550</sub> are observed when the cytochrome is adsorbed to a graphite electrode used for cyclic voltammetry (4) and similarly, a more positive potential is observed when redox titrations are performed with the cytochrome bound to the photosystem II complex (5). A more modest, but still significant, change of MP is observed for the V45L/V61L double substitution mutant of cytochrome *b*<sub>5</sub>, which in this case involved a mutational increase in heme edge exposure. The surface exposure of the heme prosthetic group of Cyt.*c*<sub>6</sub> is 6.6% as compared to the more surface-exposed Cyt.*c*<sub>550</sub> of 9.7%. Thr48 and Leu91 were chosen as mutation target sites to try to reduce heme solvent exposure and because of their involvement in the hydrogen-bonding network (Figure 1B). Thr48 and Leu91 were both mutated to an isoleucine since it has a nonpolar, longer side chain. Although heme solvent exposure has long been recognized as a major contributing factor to MP, Mao et al. (9, 10), indicate that it is probably multiple factors that lead to a change in MP where solvent exposure is concerned. They also note that typically the addition of surface groups covering the heme will raise the MP because the heme will now be buried and the MP will increase regardless of solvent. However, the T48I target, which was selected primarily to aid in covering the solvent exposed heme, did not allow for significant enough coverage to result in a change in MP upon the substitution of threonine for isoleucine.

**Axial Heme Ligand, Histidine 92.** Bishistidyl ligation tends to result in more negative MPs for the heme than Met–His ligation since methionine has a more electron-withdrawing ligand character and, therefore, tends to stabilize the reduced state relative to the more electron-donating His ligand, which tends to destabilize the reduced state thus making the MP of the bisHis coordinated heme intrinsically more negative (9, 34). The difference between bisHis and His–Met axial ligation is estimated to be in the range of ~165 mV on the basis of model complexes (28), which is consistent with previous mutagenesis studies (20, 34, 35). However, it was found that conversion of bisHis to His–Met axial ligation in the C550–H92M mutant resulted in a considerably smaller change in MP, 69 mV more positive than the anticipated ~165 mV (20, 34, 35). Indeed, the measurements of the redox potential are at variance with the corresponding His to Met mutation of Cyt.*c*<sub>550</sub> from *Thermosynechococcus elongatus*, where a 130 mV upshift in potential was observed. The different result is unlikely due to the species difference since the proteins are highly homologous in terms of both amino acid sequence and 3-D structure. What would cause the difference between recombinant *Synechocystis* C550–H92M and natively expressed *Thermosynechococcus elongatus* C550–H92M? Although, a test for thioether linkage was not described in the report of the *Thermosynechococcus elongatus* cytochrome (20), our work has shown that the

thioether linkage is formed in the natively expressed *Synechocystis* C550–H92M (36), in contrast to the present analysis of *E. coli*-expressed C550–H92M. Note that all the other forms of the recombinant Cyt.*c*<sub>550</sub> expressed in the present system did have a covalently attached heme, except for the C550–H92M mutant. Spectra for the recombinant *Synechocystis* C550–H92M were virtually unchanged, yet the natively expressed C550–H92M from *Thermosynechococcus* with the thioether linkage is red-shifted by 3 nm. Unfortunately, the natively expressed *Synechocystis* C550–H92M proved highly labile and thus recalcitrant to purification. This lability was shared by the *Thermosynechococcus* C550–H92M mutant, but in this case, the authors were successfully able to partially purify the cytochrome from detergent-solubilized PSII particles and thereby obtain the spectral and redox properties of the mutant. This strategy did not succeed for us using the *Synechocystis* preparation, presumably due to the relative ease with which mutant Cyt.*c*<sub>550</sub> is released from the mesophilic *Synechocystis* PSII compared to the thermophilic *Thermosynechococcus* PSII preparations. On the basis of the finding of the formation of the thioether linkage in the natively expressed *Synechocystis* C550–H92M, it is possible that the *Thermosynechococcus* C550–H92M mutant likewise had a thioether linkage and that the difference in MPs between the *E. coli*-expressed C550–H92M ( $E_{m7} = -185$  mV) and the natively expressed *Thermosynechococcus* C550–H92M ( $E_{m7} = -140$  mV) is due to the absence of the linkage in the *E. coli*-expressed C550–H92M ( $E_{m7} = -185$  mV). Molecular modeling indicates that the formation of the methionine ligation would likely involve a distortion of the local protein structure. Without moving the protein  $\alpha$ -carbon backbone, the Met 92–Fe distance would be 3.17 Å versus the 2.0 Å for the natural His 92–Fe distance. It is possible that the absence of the thioether linkage allows an alternate binding configuration that mitigates this apparent structural constraint and, at the same time, offsets the intrinsic increase in potential. For example, the absence of the thioether linkage may allow closer ligation of the methionine and concomitant greater closing of the binding cleft thereby excluding the solvent. Obviously, other explanations, such as reorienting of backbone dipoles, are equally possible and will require further analysis to better discriminate among them and electronic effects on the heme due to the absence of the thioether.

Pro 93 is conserved in Cyt.*c*<sub>550</sub> and was selected as a target site since it forms a conserved hydrogen bond with the (imidazole) N $\delta$  atom of His 92 (8, 22). His 92 is actually hydrogen-bonded between N $\delta$ 1 of its imidazole ring to carbonyls of Pro 93 and Lys 45 (8, 22). Molecular modeling suggests that the alanine substitution for proline does not remove the hydrogen bond; however, it may change the geometry of the hydrogen bonding, which may force a carbonyl oxygen location that either orients the imidazole differently or causes a different orientation of the backbone changing the dipole direction therefore accounting for the 19 mV upshift in redox potential.

## CONCLUSIONS

Cyt.*c*<sub>550</sub> of cyanobacterial PSII represents a unique natural example of how a protein fold that is superficially similar to many more positive *c*-type cytochromes produces a very different redox potential. The present mutagenesis analysis

points to the existence of multiple factors, including H-bond interactions and the chemical identity of the axial ligands, contributing to this difference. However, concerted mutations, perhaps mimicking the protein domain near the axial 6th ligand of the closely related but much higher potential Cyt.*c*<sub>6</sub>, may be required to address the contribution of other factors, most notably, the level of solvent exposure of the heme. From the biological perspective, Cyt.*c*<sub>550</sub> remains enigmatic since this cytochrome is not necessary for the main electron-transfer events associated with the H<sub>2</sub>O oxidation reaction catalyzed by PSII, despite the fact that it orients its heme edge to within 25 Å of the cluster of manganese ions responsible for the catalysis of this reaction. If the cytochrome is not simply an evolutionary vestige of a former electron donor to the ancestral photosynthetic reaction center complex, then one possibility is that it has a function in detoxifying reactive oxygen species that may be produced by the photochemical reactions of the reaction center. To explore this possibility, the susceptibility of the heme iron to undergo ligand exchange was tested using CO and NaN<sub>3</sub>. No such reaction was detected even if the pH was modified to enhance the protonation state of the axial His ligands. Thus, if the low-potential cytochrome does have a detoxification function, then it seems that it cannot operate by a ligand substitution reaction between the putative species and the heme iron.

## ACKNOWLEDGMENT

We thank Dr. Thony-Meyer (Mikrobiologisches Institut, Zurich, Switzerland) for allowing us to use the plasmid pEC86 and Dr. John Whitmarsh for supplying the plasmid pEC86.

## REFERENCES

1. Dolla, A., Blanchard, L., Guerlesquin, F., and Bruschi, M. (1994) The protein moiety modulates the redox potential in cytochromes *c*, *Biochimie* 76, 471–479.
2. Barker, P. D., and Ferguson, S. J. (1999) Still a puzzle: why is haem covalently attached in *c*-type cytochromes?, *Struct. Fold Des.* 7, R281–R290.
3. Holten, R. W., and Meyers, J. (1963) Cytochromes of a blue-green algae: extraction of a *c*-type with a strongly negative redox potential, *Science* 142, 234–235.
4. Vrettos, J. S., Reifler, M. J., Kievit, O., Lakshmi, K. V., de Paula, J. C., and Brudvig, G. W. (2001) Factors that determine the unusually low reduction potential of cytochrome *c*<sub>550</sub> in cyanobacterial photosystem II, *J. Biol. Inorg. Chem.* 6, 708–716.
5. Roncel, M., Boussac, A., Zurita, J. L., Bottin, H., Sugiura, M., Kirilovsky, D., and Ortega, J. M. (2003) Redox properties of the photosystem II cytochromes b559 and c550 in the cyanobacterium *Thermosynechococcus elongatus*, *J. Biol. Inorg. Chem.* 8, 206–216.
6. Navarro, J. A., Hervas, M., De la Cerda, B., and De la Rosa, M. A. (1995) Purification and physicochemical properties of the low potential cytochrome C549 from the cyanobacterium *Synechocystis* sp. PCC 6803, *Arch. Biochem. Biophys.* 318, 46–52.
7. Cho, Y. S., Wang, Q. J., Krogmann, D., and Whitmarsh, J. (1999) Extinction coefficients and midpoint potentials of cytochrome *c*(6) from the cyanobacteria *Arthrospira maxima*, *Microcystis aeruginosa*, and *Synechocystis* 6803, *Biochim. Biophys. Acta* 1413, 92–97.
8. Sawaya, M. R., Krogmann, D. W., Serag, A., Ho, K. K., Yeates, T. O., and Kerfeld, C. A. (2001) Structures of cytochrome *c*-549 and cytochrome *c*6 from the cyanobacterium *Arthrospira maxima*, *Biochemistry* 40, 9215–9225.
9. Mao, J., Hauser, K., and Gunner, M. R. (2003) How cytochromes with different folds control heme redox potentials, *Biochemistry* 42, 9829–9840.



10. Wirtz, M., Oganess, V., Zhang, X., Studer, J., and Rivera, M. (2000) Modulation of redox potential in electron transfer proteins: effects of complex formation on the active site microenvironment of cytochrome  $b_5$ , *Faraday Discuss.* 116, 221–234.
11. Thony-Meyer, L. (2002) Cytochrome  $c$  maturation: a complex pathway for a simple task?, *Biochem. Soc. Trans.* 30, 633–638.
12. Schulz, H., Fabianek, R. A., Pelliccioli, E. C., Hennecke, H., and Thony-Meyer, L. (1999) Heme transfer to the heme chaperone CcmE during cytochrome  $c$  maturation requires the CcmC protein, which may function independently of the ABC-transporter CcmAB, *Proc. Natl. Acad. Sci. U.S.A.* 96, 6462–6467.
13. Sambrook, J., Fritsch, E. F., and Maniatis, T. (1989) *Molecular Cloning: A Laboratory Manual*, 2nd ed., Cold Spring Harbor Laboratory, Cold Spring Harbor, NY.
14. Cho, Y. S., Pakrasi, H. B., and Whitmarsh, J. (2000) Cytochrome  $cM$  from *Synechocystis* 6803. Detection in cells, expression in *Escherichia coli*, purification and physical characterization, *Eur. J. Biochem.* 267, 1068–1074.
15. Ho, K. K., Ulrich, E. L., Krogmann, D. W., and Gomez-Lojero, C. (1979) Isolation of photosynthetic catalysts from cyanobacteria, *Biochim. Biophys. Acta* 545, 236–248.
16. Stankovich, M. T. (1980) An anaerobic spectroelectrochemical cell for studying the spectral and redox properties of flavoproteins, *Anal. Biochem.* 109, 295–308.
17. Bourrot, S., Sire, O., Trautwetter, A., Touze, T., Wu, L. F., Blanco, C., and Bernard, T. (2000) Glycine betaine-assisted protein folding in a *lysA* mutant of *Escherichia coli*, *J. Biol. Chem.* 275, 1050–1056.
18. Sosa-Peinado, A., Mustafi, D., and Makinen, M. W. (2000) Overexpression and biosynthetic deuterium enrichment of TEM-1 beta-lactamase for structural characterization by magnetic resonance methods, *Protein Expression Purif.* 19, 235–245.
19. Rosell, F. I., and Mauk, A. G. (2002) Spectroscopic properties of a mitochondrial cytochrome  $C$  with a single thioether bond to the heme prosthetic group, *Biochemistry* 41, 7811–7818.
20. Kirilovsky, D., Roncel, M., Boussac, A., Wilson, A., Zurita, J. L., Ducruet, J. M., Bottin, H., Sugiura, M., Ortega, J. M., and Rutherford, A. W. (2004) Cytochrome  $c550$  in the Cyanobacterium *Thermosynechococcus elongatus*: study of redox mutants, *J. Biol. Chem.* 279, 52869–52880.
21. Shen, J. R., Ikeuchi, M., and Inoue, Y. (1992) Stoichiometric association of extrinsic cytochrome  $c550$  and 12 kDa protein with a highly purified oxygen evolving photosystem II core complex from *Synechococcus vulcanus*, *FEBS Lett.* 301, 145–149.
22. Frazao, C., Enguita, F. J., Coelho, R., Sheldrick, G. M., Navarro, J. A., Hervas, M., De la Rosa, M. A., and Carrondo, M. A. (2001) Crystal structure of low-potential cytochrome  $c549$  from *Synechocystis* sp. PCC 6803 at 1.21 Å resolution, *J. Biol. Inorg. Chem.* 6, 324–332.
23. Thony-Meyer, L., Kunzler, P., and Hennecke, H. (1996) Requirements for maturation of *Bradyrhizobium japonicum* cytochrome  $c550$  in *Escherichia coli*, *Eur. J. Biochem.* 235, 754–761.
24. Thony-Meyer, L. (2000) Haem-polypeptide interactions during cytochrome  $c$  maturation, *Biochim. Biophys. Acta* 1459, 316–324.
25. Tomlinson, E. J., and Ferguson, S. J. (2000) Loss of either of the two heme-binding cysteines from a class I  $c$ -type cytochrome has a surprisingly small effect on physicochemical properties, *J. Biol. Chem.* 275, 32530–32534.
26. Mauk, M. R., Mauk, A. G., Chen, Y. L., and Douglas, D. J. (2002) Tandem mass spectrometry of protein–protein complexes: cytochrome  $c$ –cytochrome  $b_5$ , *J. Am. Soc. Mass Spectrom.* 13, 59–71.
27. Rivera, M., Barillas-Mury, C., Christensen, K. A., Little, J. W., Wells, M. A., and Walker, F. A. (1992) Gene synthesis, bacterial expression, and  $^1H$  NMR spectroscopic studies of the rat outer mitochondrial membrane cytochrome  $b_5$ , *Biochemistry* 31, 12233–12240.
28. Moore, G. R., and Pettigrew, G. W. (1990) *Cytochromes c. Evolutionary, Structural, and Physicochemical Aspects*, Springer, Berlin, Heidelberg, and New York.
29. Reid, L. S., Mauk, M. R., and Mauk, A. G. (1984) Role of heme propionate groups in cytochrome  $b_5$  electron transfer, *J. Am. Chem. Soc.* 106, 2182–2185.
30. Rivera, M., Seetharaman, R., Girdhar, D., Wirtz, M., Zhang, X., Wang, X., and White, S. (1998) The reduction potential of cytochrome  $b_5$  is modulated by its exposed heme edge, *Biochemistry* 37, 1485–1494.
31. Kerfeld, C. A., and Krogmann, D. (1998) Photosynthetic cytochromes  $c$  in cyanobacteria, algae, and plants. *Annu. Rev. Plant Physiol. Plant Mol. Biol.* 49, 397–425.
32. Cutler, R. L., Davies, A. M., Creighton, S., Warshel, A., Moore, G. R., Smith, M., and Mauk, A. G. (1989) Role of arginine-38 in regulation of the cytochrome  $c$  oxidation–reduction equilibrium, *Biochemistry* 28, 3188–3197.
33. Kassner, R. J. (1972) Effects of nonpolar environments on the redox potentials of heme complexes, *Proc. Natl. Acad. Sci. U.S.A.* 69, 2263–2267.
34. Raphael, A. L., and Gray, H. B. (1989) Axial ligand replacement in horse heart cytochrome  $c$  by semisynthesis, *Proteins* 6, 338–340.
35. Miller, G. T., Zhang, B., Hardman, J. K., and Timkovich, R. (2000) Converting a  $c$ -type to a  $b$ -type cytochrome: Met61 to His61 mutant of *Pseudomonas* cytochrome  $c$ -551, *Biochemistry* 39, 9010–9017.
36. Li, Z., Andrews, H., Eaton-Rye, J. J., and Burnap, R. L. (2004) In situ effects of mutations of the extrinsic cytochrome  $c550$  of photosystem II in *Synechocystis* sp. PCC6803, *Biochemistry* 43, 14161–14170.

BI0500473